Journal of Physics: Conference Series **157** (2009) 012008 doi:10.1088/1742-6596/157/1/012008

Time resolved QCLAS measurements in pulsed cc-rf CF_4/H_2 plasmas

S Stepanov[1], S Welzel[2], J Röpcke[2] and J Meichsner[1]

[1] Institute of Physics, University of Greifswald, Felix-Hausdorff-Str. 6, D-17489, Greifswald, Germany

[2] Leibniz Institute for Plasma Science and Technology, Felix-Hausdorff-Str. 2, D-17489, Greifswald, Germany

E-mail: stepanov@physik.uni-greifswald.de

Abstract. Fluorocarbon containing capacitively coupled radio frequency (cc-rf) plasmas are widely used in technical applications and as model systems for fundamental investigations of complex plasmas. Absorption spectroscopy based on pulsed quantum cascade lasers (QCL) was applied in the mid-IR spectral range of 1269-1275 cm^{-1}. Absolute densities of the precursor molecule CF_4 and of the stable product C_3F_8 were measured with a time resolution of up to 1 ms in pulsed CF_4/H_2 asymmetrical cc-rf (13.56 MHz) discharges. For this purpose both the non-negligible temperature dependence of the absorption coefficients and the interference of the absorption features of CF_4 and C_3F_8 had to be taken into account in the target spectral range. Therefore, at two different spectral positions composite absorption spectra were acquired under the same plasma conditions in order to discriminate between CF_4 and C_3F_8 contributions. A total consumption of ~ 12 % was observed for CF_4 during a 1 s plasma pulse, whereas C_3F_8 appeared to be produced mainly from amorphous fluorocarbon layers deposited at the reactor walls. A gas temperature increase by ~ 100 K in the plasma pulse was estimated from the measurements. Additionally, not yet identified unresolved absorption (potentially from the excited CF_4 molecule) was found during the 'on-phase'.

1. Introduction

Manifold applications of fluorocarbon plasmas and their increasing importance in industry motivate fundamental investigations of these complex plasmas. Pulsing of the discharge can be used as an additional parameter for process control, since many plasma parameters, e.g. densities and temperatures, become time dependent [1, 2]. Therefore, absolute concentrations of key stable and transient species measured in pulsed plasmas with a high time resolution are essential for a better understanding of the plasma chemistry and kinetics in these plasmas.

Within the last decades absorption spectroscopy (AS) has been established as a suitable diagnostic tool for monitoring absolute ground state number densities in plasmas. For years tunable lead salt diode lasers (TDL) have been used as light sources in the mid infrared (IR) spectral range between 3 and 20 μm, where characteristic absorption lines of many molecular species are normally located [3, 4]. In particular infrared tunable diode laser absorption spectroscopy (IR-TDLAS) has been successfully applied for time resolved studies of CF-, CF_2-radicals and C_2F_4 as a stable reaction product in capacitively coupled radio frequency (rf) CF_4/H_2 pulsed plasmas (13.56 MHz) [1].

Furthermore, based on the simultaneous monitoring of selected absorption lines, a novel method was developed for the time resolved determination of the rotational temperature of the CF_2 radical within a single plasma pulse [2]. Recently, quantum cascade lasers (QCL) have become available as alternative light sources in the mid-IR spectral range [5, 6] Distributed feedback (DFB)-QCLs combine narrow bandwidth single-frequency operation with continuous tunability over several wavenumbers, and average powers over a mW. Hence they are not only used for highly sensitive trace gas spectrometers in various fields of applications, e.g., isotope measurements [7], atmospheric sensing [8], explosives detection [9] or breath analysis, but also being increasingly employed for plasma diagnostics [10-12] or plasma process monitoring [13]. In particular pulsed QCLs offer the opportunity to achieve a much higher time resolution compared to lead salt laser systems [11]. If a relatively long QCL pulse of a few 100 ns is applied a full absorption spectrum of up to a few cm^{-1} can be acquired within the laser pulse [14]. The time resolution is thus theoretically limited to the pulse length of the laser.

In this contribution a study on pulsed CF_4/H_2 capacitively coupled rf discharges is reported focussing on the time resolved measurements of the absolute concentrations of stable molecules. Therefore quantum cascade laser absorption spectroscopy (QCLAS) employing a pulsed room-temperature QCL emitting at 7.86 μm has been applied. The QCL spectrometer was co-aligned to an existing TDL setup [2] and time resolved concentration measurements have been performed on CF_4 and C_3F_8. The experimental arrangement and the data handling approach are described in section 2. The results are presented and discussed (also in terms of the alternating gas temperature in the discharge) in section 3 and summarised in section 4.

2. Experimental set-up and data handling

2.1. Discharge set-up

The experimental arrangement is shown schematically in figure 1. The discharge was created in a cylindrical stainless steel vacuum chamber with a total volume of ca. 20 l. A cylindrical copper block of about 8 cm in diameter was placed in the centre of the chamber and capacitively coupled with the 13.56 MHz rf power generator (ENI ACG-5) by means of a matching network (ENI MW-5). The chamber walls were grounded resulting in a highly asymmetrical rf discharge. The power generator was pulsed by a master pulse generator (BNG 555) with a period of 3 s. The process gases CF_4 and H_2 were fed into the reactor at a flow rate of 7 and 3 sccm, respectively, through small holes in the shielding around the powered electrode. The total pressure in the chamber (5-25 Pa) was measured with a capacitance manometer (MKS pressure transducer type 122A) and controlled independently from the constant gas flow rates. For that the pumping speed of the rotary pump (Leybold, D 25 BCS) was regulated by means of a throttle valve controller (MKS pressure controller type 652) which also enabled the pressure to be recorded with a time resolution of ~ 0.25 s.

2.2. Spectroscopic set-up

The QCLAS measurements of CF_4 and C_3F_8 were carried out in the spectral range of 1269-1275 cm^{-1} using a pulsed thermoelectrically (TE) cooled QCL (Alpes Lasers) housed in a QCL measurement and control system (Q-MACS, neoplas control) [15]. The QCL was operated with 300 ns pulses at two different heat sink temperatures and therefore provided spectral scans centered around 1271 cm^{-1} and 1274 cm^{-1}, each of ~ 1 cm^{-1} spectral coverage [16]. The light emitted by the QCL was guided in a double pass through the reactor approximately 4 cm above the rf electrode (figure 1). The total absorption path length through the plasma chamber was ~ 90 cm. The transmitted signal was focused onto a fast TE cooled detector (PDI-3TE-10/12, VIGO) followed by a fast preamplifier (neoplas control) and a fast digitizing oscilloscope (WR 104Xi, LeCroy). In order to generate a stable trigger for the data acquisition and to avoid any jitter between the driving electronics and the optical output, a small portion of the QCL beam was deflected using a ZnSe beam splitter onto a second fast TE cooled detector in a reference path. The rising edge of the reference signal served as trigger for the acquisition of the QCL signal transmitted through the reactor.

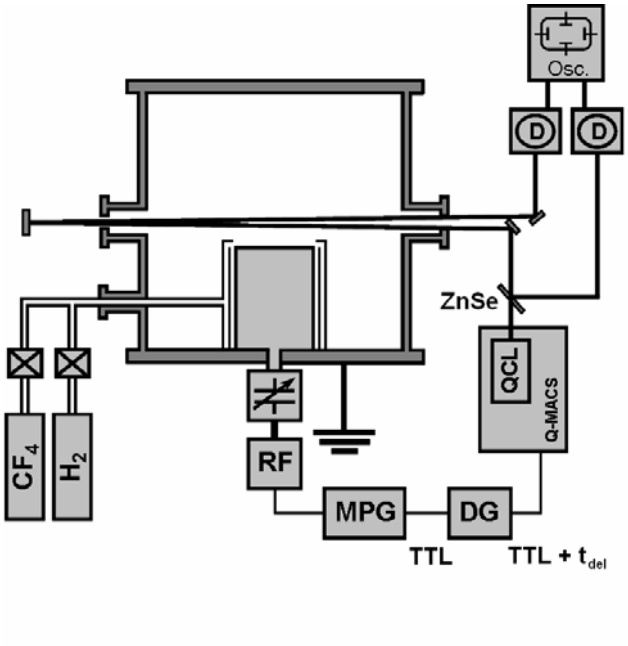

Figure 1. Experimental set-up (MPG - master pulse generator, DG - delay generator, RF – rf power generator, D – detector with preamplifier, Osc. - oscilloscope).

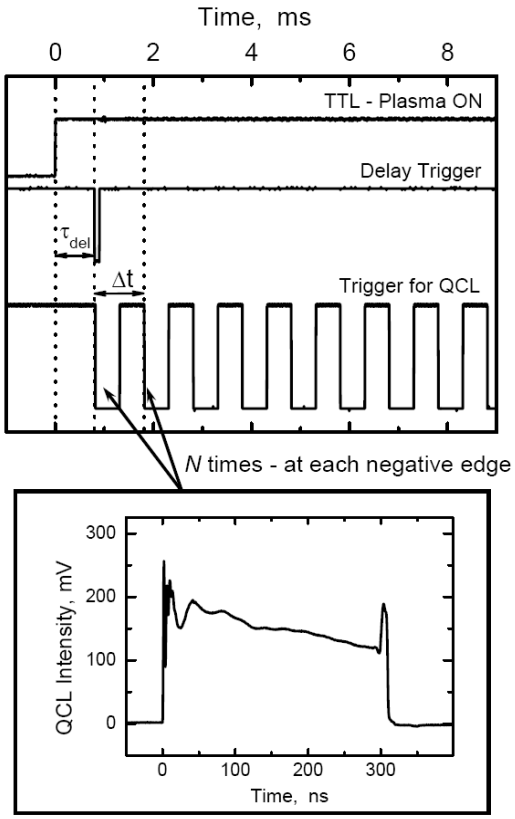

Figure 2. Trigger scheme for the time resolved data acquisition after igniting the discharge. *Upper:* A master (TTL) pulse triggers the discharge and *N* subsequent QCL pulses (via a frequency generator). *Lower:* Sample spectrum of a single QCL pulse.

To synchronize the QCL pulses with the discharge, a gate TTL trigger of the master pulse generator was used (figure 2). This master gate signal determined the 'plasma-on' phase and realized simultaneously the master trigger for all subsequently recorded QCL spectra relative to the plasma pulse. A delay generator launched a sequence of *N* short trigger pulses for the QCL with a delay time of τ_{del} after the master gate signal (figure 2). This burst of the QCL trigger events was realized by a frequency generator (Hewlett Packard). The repetition frequency of these *N* short pulses defined the time resolution of the measurements Δt. Thus, the sampling of the plasma pulse by means of QCL pulses was determined by three parameters τ_{del}, *N* and Δt, respectively. Typically, a burst of $N = 600$ pulses with a time resolution of $\Delta t = 5$ ms, launched $\tau_{del} = 500$ ns after the master gate signal, was used to map the entire plasma pulse. For a more detailed analysis of the plasma ignition or early afterglow a better time resolution of $\Delta t = 1$ ms was chosen. Finally, to increase the signal to noise ratio, 25 of such sequences (i.e. from 25 different plasma cycles) were recorded and averaged in a first step of the post data treatment yielding *N* averaged spectra.

For further data analysis the signal without any absorbing species (base line) and with a germanium etalon (25.4 mm, 0.0485 cm^{-1} free spectral range) in the beam path were recorded after each series of measurements. N_2O and CH_4 were used as reference gases for absolute calibration of the frequency scale.

2.3. Data handling

The number density n of the absorbing species can be derived from the relationship between the incident (I_0) and transmitted (I) laser intensity, based on Beer-Lambert's law:

$$I(\nu) = I_0(\nu)e^{-n\sigma(\nu,T)L} \tag{1}$$

where L is the absorption length and $\sigma(\nu,T)$ is the temperature dependent absorption cross section at wavenumber ν. The complex spectra of CF_4 and C_3F_8 measured within the target spectral range at the current low pressure conditions were found to be affected by the rapidly chirped QCL pulses (so called 'rapid passage effect', [17]). Therefore calibration of the absorption cross sections was required. Following an approach similar to Stancu *et al* [13] an effective integrated absorption cross section σ^{eff} was defined:

$$\sigma_{eff} = \frac{1}{n \cdot L} \ln \frac{\langle I_0(\nu) \rangle}{\langle I(\nu) \rangle} = \frac{1}{n \cdot L} \ln\left(\frac{A_0}{A}\right) \tag{2}$$

where $\langle ... \rangle$ (further denoted as A) is the signal averaged over a distinct narrow spectral range. Further details on the σ_{eff} definition and calibration procedure including a detailed analysis of the temperature dependence $\sigma_{eff}(T)$ can be found in [16].

Since the spectral features of CF_4 and C_3F_8 (further denoted with index $k = 1$ and 2, respectively) were found to interfere in the target spectral range, the number density n_k of one of these molecules could not directly be determined from a single plasma measurement. Each acquired spectrum might be composed of contributions from both molecules. However, the significantly different dependence of the CF_4 and C_3F_8 absorption cross sections on ν provides a means to discriminate between the two species of interest. Therefore, time resolved measurements were carried out under identical plasma conditions at two separate spectral positions ν_j around 1271 cm^{-1} and 1274 cm^{-1}, respectively, where the ratio of the absorption cross sections σ_k^{eff} for CF_4 and C_3F_8 was considerably different [16]. After the initial averaging over 25 plasma cycles the time dependent absorption $I(\nu_j,t_i)$ at the considered spectral positions is obtained. Next, for each time step t_i a system of two nonlinear equations had to be solved numerically using the $\sigma_k^{eff}(\nu_j,T(t_i))$ values calculated for the current temperature $T(t_i)$ in the plasma (cf. Appendix). Finally, this yielded the time dependent absolute number densities $n_k(t_i)$ for CF_4 and C_3F_8 under considered plasma conditions:

$$I(\nu_j, t_i) \xrightarrow{\sigma_k^{eff}(\nu_j,T(t_i))} n_k(t_i) \quad (t_i = 1...N). \tag{3}$$

3. Results and discussion

3.1. Properties of the pulsed discharge

For further interpretation of the performed absorption measurements external discharge parameters were investigated in preliminary experiments. Figure 3 shows a typical rf voltage sample at the beginning of the 'plasma-on' phase obtained by averaging over 25 successive plasma cycles. Typically, ~ 1 ms after the initial trigger to the rf power generator a short and unstable plasma burst was observed, followed by ~ 0.5 ms where the plasma was absent. A second onset, ~ 1.5 ms after the initial trigger, led to stable discharge conditions. Thus, experiments with the best time resolution were carried out with Δt = 1 ms. For all other cases Δt = 5 ms was chosen.

The typical behaviour of the total pressure during a plasma cycle is shown in figure 4. The response time of the throttle valve controller was not fast enough to keep the pressure inside the chamber at a constant level. Furthermore the time resolution of the data acquisition from the controller was limited to 0.2 s resulting in a flattened slope of the pressure at the transition points. Nevertheless, the pressure increase of about 30 % can qualitatively be understood as an upper limit of the temperature increase

during the 'plasma-on' phase compared to the room temperature level in the 'plasma-off' phase. This approximation leads to a gas temperature of ~ 390 K in the plasma which was used for all further calculations. Moreover, this estimation correlates with rotational temperature values found under similar conditions for CF_2 radicals in plasmas [2].

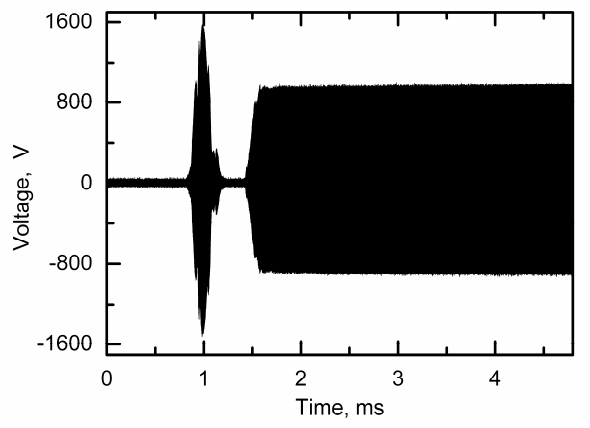

Figure 3. Typical rf sample measured at the beginning of the 'plasma-on' phase (10 Pa, 7 sccm CF_4 + 3 sccm H_2, 100 W).

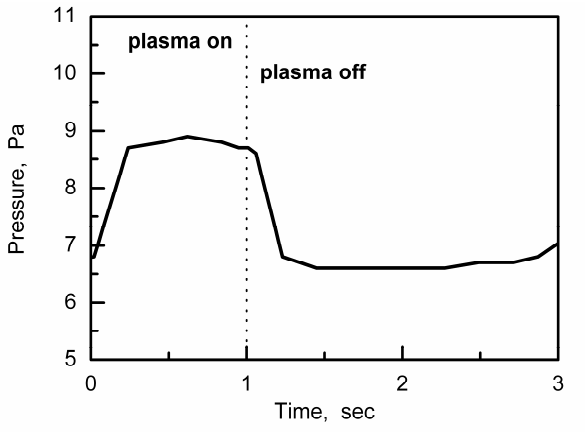

Figure 4. Total pressure change measured over a full plasma cycle (7 sccm CF_4 + 3 sccm H_2, 100 W).

3.2. Time resolved analysis of species concentration

Figure 5 shows an example for the absorbance $\ln(A_0/A)$ measured at the two studied spectral positions ν_j under identical plasma conditions. In both time traces a steep increase of the absorption in the 'plasma-on' is observed, whereas the behaviour during the plasma pulse is slightly different: at 1274 cm^{-1} where CF_4 has its strongest absorption cross section for the two positions ν_j the absorption is gradually decreasing during the plasma pulse (curve b) whereas at 1271 cm^{-1} the absorption is almost constant (curve a). If only CF_4 features were considered a decrease of the absorption values due to the conversion of the precursor gas would be expected. In the 'plasma-off' phase the absorption increases slightly at 1274 cm^{-1}, but is almost constant at 1271 cm^{-1}. Thus this example demonstrates that the individual temperature dependences of the absorption cross sections and contributions from plasma produced species to the absorption have to be taken into account for the further analysis. More detailed measurements with a higher time resolution (not shown here) at the transition points between 'plasma-on' and 'off' phase also revealed that: i) the ~ 1 ms delay of the power input into the plasma after the trigger (figure 3) was also present in the IR data, and ii) the rapid changes in the absorption at the beginning and the end of the plasma pulse occurred mostly within 25 ms.

Potential transient and stable molecules that might be detected in the CF_4/H_2 plasma are CF, CF_2 CF_3 as well as CHF_3, C_2F_4, C_2F_6 and C_3F_8. Higher fluorocarbon molecules were not very likely to be produced and present in the gas phase. Except for C_3F_8 none of the mentioned stable $C_xH_yF_z$ molecules showed absorption features in the target spectral range. CF_2 exhibits no absorption lines in the considered range. The absorption features of CF and CF_3 would be too weak to cause such a steeply rising edge as in figure 5. Moreover, the absorption lines of the CF_x radicals are typically well-resolved in a spectrum. As a consequence, $\ln(A_0/A)$ should have different values for distinct spectral micro-windows ν_j depending on whether a CF_x radical line is included or not. However such behaviour was not observed. Hence, the measured broadband absorption in the target spectral range is expected to be caused by CF_4 and C_3F_8.

Following equation (3) and considering the temperature dependence of the absorption cross sections the data handling procedure yielded the number densities of CF_4 and C_3F_8. The influence of the gas temperature in the 'on-phase' on the calculated number densities was checked separately to

study their sensitivity on this input parameter. For a temperature range of 350 to 430 K no significant difference in the general trends was found. However, the value of 390 K which was estimated in section 3.1 fits best because any sharp change in n_1 is absent in this case at the 'on-off' transition. The number densities of CF_4 and C_3F_8 obtained for $T = 390$ K are shown in figure 6. A gradual increase of CF_4 in the order of 1.2×10^{14} cm^{-3} is observed during the 'plasma-off' phase. This can be attributed to the unfinished gas replacement because the residence time was estimated to be ~ 12 s for the present experimental conditions. In the 'on-phase' the initial precursor concentration decreases by ~ 12 % due to both dissociation and conversion processes. Since an additional underlying absorption of C_3F_8 was assumed for the data analysis, an immediate increase of its density n_2 from zero (or noise) level in the 'off-phase' up to 2.8×10^{14} cm^{-3} during the discharge is deduced.

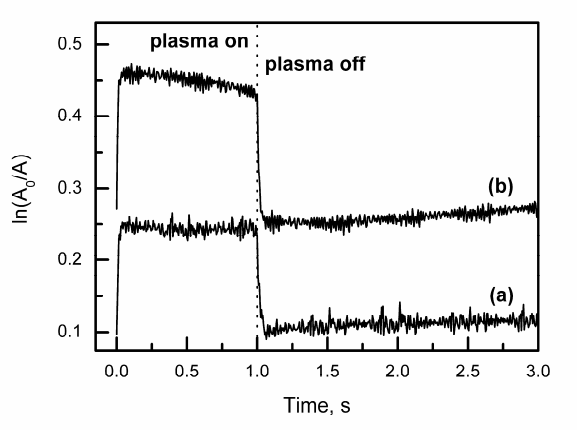

Figure 5. The ratio of the signal intensities $\ln(A_0/A)$ measured in pulsed plasma at: (a) 1271 cm^{-1} and (b) 1274 cm^{-1} (10 Pa, 7 sccm CF_4 + 3 sccm H_2, 100 W).

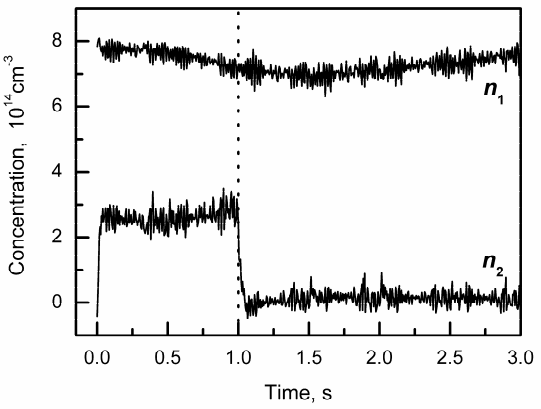

Figure 6. Time resolved absolute number densities n_1 (CF_4) and n_2 (C_3F_8) obtained for $T = 390$ K (10 Pa, 7 sccm CF_4 + 3 sccm H_2, 100 W).

The carbon-fluorine content which follows from the calculated number densities of the precursor molecule CF_4 and the product C_3F_8 (figure 6) clearly exceeds the initial content in the feed gas flow. This suggests an additional non-negligible fluorocarbon source and its conversion in the gas phase. Thus, amorphous fluorocarbon (a:C-F) layers deposited at the chamber walls during previous experiments may mainly contribute to the C_3F_8 formation in figure 6. After switching the plasma off the production via this channel stops. Diffusion losses and subsequent chemical reactions lead therefore to the sudden drop of n_2. However, the time scale of less than 100 ms observed for this decrease in n_2 is almost one order of magnitude smaller than typical values found for other stable products [1]. Moreover, if the calculated number density of C_3F_8 were present, the gas phase would also contain a significant number of C_2F_6 molecules [18, 19] which in turn would further increase the excess of fluorocarbons compared to the initial feed gas flow. Further effects or species may therefore contribute to the observed time trace of n_2.

In order to identify the main stable products and estimate their number densities, FTIR spectra of the 'off-phase' gas composition were recorded and compared with reference spectra which were previously acquired for calibration purposes. A glass cell attached to the plasma reactor was used to extract a sample of the gas phase after discharge operation. Next, the measurements were performed *ex-situ* by means of a FTIR spectrometer (Bruker Vertex 80V). Apart from the precursor molecule CF_4 the stable compounds C_2F_6, C_3F_8, CHF_3 and HF were identified. Although these complimentary measurements cannot directly be compared with the QCLAS results, they provide a means to assess the trends found in the time-resolved QCL experiments. The number densities of C_2F_6 and C_3F_8 in the sample cell were determined from a linear fit to calibration spectra and found to be of 1.8×10^{14} cm^{-3}

and 0.4×10^{14} cm^{-3}, respectively. Since the present C_3F_8 detection limit estimated from the peak-to-peak noise level is of the same order (0.3×10^{14} cm^{-3}), the C_3F_8 density during the 'off-phase' is just below this value which also explains the observed "zero-signal" of n_2. Furthermore, if the C_2F_6 estimate is considered in respect to the calculated 'on-phase' value for n_2 (which is almost twice as big) and its time dependence, another short-lived molecule or absorption feature should be included in the data analysis. Since potential radicals exhibit no (broad-band) absorption in the present spectral range, CF_4 hot bands may be the most reasonable absorption feature [18]. Unfortunately, such an influence cannot be calibrated and included in the analysis using the present methods. Further investigations are therefore necessary to discriminate the obviously non-negligible contribution of excited CF_4 from other stable molecules of interest.

4. Summary and conclusions

The absolute number densities of CF_4 and C_3F_8 have been measured in pulsed CF_4/H_2 rf plasmas by means of time resolved QCLAS with a time resolution of typically 5 ms. In order to deconvolve the composed absorption spectra with main contributions from at least two stable species with broadband, unresolved absorption, two spectra had to be acquired under the same plasma conditions in two separate spectral micro-windows. A sensitivity analysis of the data retrieval procedure confirmed the gas temperature value of 390 K which was approximated initially from the pressure increase in the 'plasma-on' phase. The concentration of the CF_4 precursor molecule decreased by ~ 12 % during the 'on' phase, whereas the suggested C_3F_8 concentration clearly increased above the noise level and immediately followed the discharge pulse. In particular the latter fact is unexpected, since, even under the assumption that C_3F_8 might be formed in plasma from amorphous fluorocarbon layers at the chamber walls, the observed rapid decrease of C_3F_8 in the 'off-phase' was not expected for a stable molecule.

Accompanying FTIR test measurements revealed the presence of C_3F_8 in the 'off-phase' gas composition, but in the order of the QCLAS detection limit (~ 0.3×10^{14} cm^{-3}). By means of applied methods it is not feasible to distinguish between C_3F_8 and other not yet considered molecules (e.g. CF_4 hot bands) during the 'on-phase'. However, the C_2F_6 number densities resulting from the FTIR spectra analysis and the carbon-fluorine content estimated for the gas phase indicate a non-negligible absorption of excited CF_4. Further investigations are therefore necessary to quantify its contribution and the actual C_3F_8 number density, in particular during the 'on-phase'.

Acknowledgements

This work was supported by the German Research Foundation (DFG) within the framework of the Collaborative Research Centre Transregio 24 ‘Fundamentals of Complex Plasmas’ (SFB-TR 24), projects B2 and B5. The authors thank D Gött, P Druckrey, U Meißner, S Saß, C Senske and F Weichbrodt for valuable technical assistance.

Appendix

If an absorption spectrum of a gas mixture is measured, the absorption from each distinct molecule can be described separately by means of equation (1). In the case of contributions from two molecules (index $k = 1$ or 2) the total transmitted signal A^j for both considered spectral ranges $j = 1$ or 2 would be

$$A^1 = A^{11} + A^{12} - A_0^1 \tag{A1}$$

$$A^2 = A^{21} + A^{22} - A_0^2 \tag{A2}$$

where A^{jk} denotes the transmitted intensity in the spectral range j for molecule k and $A^j{}_0$ describes the base line for the range j. The number densities n_k can be derived from

$$n_1 = \frac{1}{\sigma_{eff}^{11} \cdot L} \ln\left(\frac{A_0^1}{A^{11}}\right) = \frac{1}{\sigma_{eff}^{21} \cdot L} \ln\left(\frac{A_0^2}{A^{21}}\right) \tag{A3}$$

$$n_2 = \frac{1}{\sigma_{eff}^{12} \cdot L} \ln\left(\frac{A_0^1}{A^{12}}\right) = \frac{1}{\sigma_{eff}^{22} \cdot L} \ln\left(\frac{A_0^2}{A^{22}}\right) \tag{A4}$$

with the effective absorption cross sections σ_{eff}^{jk}. Rearranging equations (A1 - A4) yields a system of two nonlinear equations for two unknown number densities n_1 and n_2

$$\begin{aligned} 1 + \frac{A^1}{A_0^1} &= \exp(-\sigma_{eff}^{11} \cdot L \cdot n_1) + \exp(-\sigma_{eff}^{12} \cdot L \cdot n_2) \\ 1 + \frac{A^2}{A_0^2} &= \exp(-\sigma_{eff}^{21} \cdot L \cdot n_1) + \exp(-\sigma_{eff}^{22} \cdot L \cdot n_2) \end{aligned} \tag{A5}$$

This system can be solved numerically, e.g., with a custom made LabVIEW program in our case, providing for the 4 different and temperature dependent absorption cross sections σ_{eff}^{jk} are known or have been calibrated. Alternatively, (A5) can be rearranged further

$$1 + \frac{A^2}{A_0^2} = \exp(-\sigma_{eff}^{21} \cdot L \cdot n_1) + \left[\left(1 + \frac{A^1}{A_0^1}\right) - \exp(-\sigma_{eff}^{11} \cdot L \cdot n_1)\right]^{\frac{\sigma_{eff}^{22}}{\sigma_{eff}^{12}}} \tag{A6}$$

and is now only a function of n_1 which can be numerically determined while n_2 follows via (A5). Both numerical approaches have been successfully checked. In this context the values I and A (as an integral of I over a spectral micro-window) were used synonymously, since these values are always used relative to the corresponding base line I_0 or A_0, i.e. A can be also considered as an averaged value for I.

References

[1] Gabriel O, Stepanov S and Meichsner J 2007 *J. Phys.* D: *Appl. Phys.* **40** 7383-91
[2] Gabriel O, Stepanov S, Pfafferott M and Meichsner J 2006 *Plasma Sources Sci. Technol.* **15** 858-64
[3] Röpcke J, Mechold L, Käning M, Anders J, Wienhold F G, Nelson D and Zahniser M 2000 *Rev. Sci. Instrum.* **71** 3706-10
[4] Eng R S, Butler J F and Linden K J 1980 *Opt. Eng.* **19** 945-60
[5] Faist J, Capasso F, Sivco D L, Sirtori C, Hutchinson A L and Cho A 1994 *Science* **264**, 553
[6] Beck M, Hofstetter D, Aellen T, Faist J, Oesterle U, Ilegems M, Gini E and Melchior H 2002 *Science* **295** 301
[7] Tuzson B, Mohn J, Zeeman M J, Werner R A, Eugster W, Zahniser M S, Nelson D D, McManus J B and Emmenegger L 2008 *Appl. Phys.* B **92** 451
[8] Hay K G, Wright S, Duxbury G, Langford N 2008 *Appl. Phys.* B **90** 329
[9] Bauer C, Sharma A K, Willer U, Burgmeier J, Braunschweig B, Schade W, Blaser S, Hvozdara L, Müller A and Holl G 2008 *Appl. Phys.* B **92** 327
[10] Cheesman A, Smith J A, Ashfold M N R, Langford N, Wright S and Duxbury G 2006 *J. Phys. Chem.* A **110** 2821
[11] Welzel S, Gatilova L, Röpcke J and Rousseau A 2007 *Plasma Sources Sci. Technol.* **16** 822-31
[12] van Helden J H, Horrocks S J and Ritchie G A D 2008 *Appl. Phys. Lett.* **92** 081506

[13] Stancu G, Lang N, Röpcke J, Reinicke M, Steinbach A and Wege S 2007 *Chem. Vap. Deposition* **13** 351-60
[14] Beyer T, Braun M and Lambrecht A 2003 *Journ. Appl. Phys.* **93** 3158
[15] Röpcke J, Lombardi G, Rousseau A and Davies P B 2006 *Plasma Sources Sci. Technol.* **15** 148
[16] Welzel S, Stepanov S, Meichsner J and Röpcke J 2008 *J.Phys.: Conf. Ser.* submitted
[17] Duxbury G, Langford N, McCulloch M T and Wright S 2005 *Chem. Soc. Rev.* **34** 921
[18] Cruden B A, Rao M V V S, Sharma S P and Meyyappan M 2002 *Plasma Sources Sci. Technol.* **11** 77-90
[19] O'Neill J A, Singh J and Gifford G G 1990 *J. Vac. Sci. Technol.* **A8** 1716